N-acetyl-*S*-(*p*-chlorophenylcarbamoyl)cysteine induces mitochondrial-mediated apoptosis and suppresses migration in melanoma cells

WEI CHEN[1,2], ZHIMING JIANG[1,2], XIAOYING ZHANG[3], JIANGUO FENG[1,2] and YUTIAN LING[1]

[1]Zhejiang Cancer Research Institute, Zhejiang Cancer Hospital, Zhejiang Cancer Center, Hangzhou, Zhejiang 310022; [2]Zhejiang Key Laboratory of Diagnosis and Treatment Technology on Thoracic Oncology (Lung and Esophagus), Hangzhou, Zhejiang 310022; [3]ACEA Bio Co., Ltd., Hangzhou, Zhejiang 310030, P.R. China

Received June 6, 2015; Accepted August 6, 2015

DOI: 10.3892/or.2015.4267

Abstract. We previously reported that *N*-acetyl-*S*-(*p*-chlorophenylcarbamoyl)cysteine (NACC) induces apoptosis in human melanoma UACC-62 cells. In the present study, the molecular mechanism of NACC-induced apoptosis in melanoma cells was investigated. Briefly, the apoptosis triggered by NACC was confirmed in UACC-62 cells for shorter treatment periods. Increased activities of caspase-3 and caspase-9 but not caspase-8 were observed in the cell lysates. Western blotting showed that the pro-apoptotic protein Bax was upregulated and the anti-apoptotic protein Mcl-1 was downregulated and cytochrome *c* (Cyto *c*) was released into the cytosol. Flow cytometric analysis demonstrated that NACC induced significant mitochondrial membrane potential disruption. Significant increases in the generation of reactive oxygen species (ROS) and cytosolic calcium elevation were also observed. However, opening of the mitochondrial permeability transition pore which could be involved in Cyto *c* leakage from mitochondria was found to be unaffected by NACC. Taken together, all the results presented in this study including apoptotic induction, activation of the caspase-3 and -9 cascade, upregulation of Bax, downregulation of Mcl-1, Cyto *c* release from the mitochondria, mitochondrial membrane potential depletion, ROS production and cytosolic calcium elevation demonstrated that NACC triggered apoptosis in the UACC-62 cells via the mitochondrial-dependent pathway. Melanoma is well-known as an aggressive and highly metastatic disease. In this study, we also investigated the effects of NACC on the migration of UACC-62 cells using the xCELLigence system. The results revealed that *in vitro* NACC is capable of inhibiting the migration of melanoma cells.

Correspondence to: Dr Wei Chen, Zhejiang Cancer Research Institute, Zhejiang Cancer Hospital, Zhejiang Cancer Center, 38 Guangji Road, Hangzhou, Zhejiang 310022, P.R. China
E-mail: chenwei@zjcc.org.cn

Key words: NACC, apoptosis, melanoma, mitochondrial pathway, migration, reactive oxygen species, caspase, mitochondrial permeability transition pore

Introduction

Malignant melanoma is aggressive and therapy-resistant (1), thus advanced and metastatic melanoma is almost uniformly fatal. Patients with advanced melanoma have a short median survival of 6-9 months (2). Melanoma is becoming more common and its incidence has risen dramatically worldwide in Caucasian populations (3,4).

It is known that melanoma cells become resistant to chemotherapeutic agents and escape from death through inactivation of apoptosis (5). Apoptosis is a crucial event in the cytotoxicity induced by anticancer agents (6). The role of apoptosis in the cytotoxicity of anticancer agents has become more and more clear (7). Apoptosis occurs via two pathways, the death receptor-dependent (extrinsic) pathway or the independent (intrinsic or mitochondrial) pathway (8). The mitochondrial pathway of apoptosis is initiated by downregulation of anti-apoptotic proteins (Bcl-2 family members) and upregulation of pro-apoptotic proteins (Bax and Bad). Several changes in mitochondrial biogenesis and function were found to be associated with the commitment to intrinsic apoptosis. The loss of mitochondrial transmembrane potential is responsible for changes in mitochondrial biogenesis and activity resulting in the opening of mitochondrial permeability transition pores (PTPs) to release cytochrome *c* (Cyto *c*) which eventually activates caspase-9 and caspase-3 and subsequent cell death. Translocation of Cyto *c* has been considered as a crucial step in the activation of the apoptotic machinery (9,10). On the other hand, Cyto *c* release from mitochondria appears to be largely mediated by direct or indirect reactive oxygen species (ROS) action (10). The involvement of calcium in cell death has been recognized very early in the history of apoptosis. Elevation of cytosolic calcium both occurs at early and late stages of the apoptotic pathways and is considered to be the final common pathway of all types of cell death (11).

In previous studies, we reported that *N*-acetyl-*S*-(*p*-chloro phenylcarbamoyl)cysteine (NACC) and its analogs are a novel class of anticancer agents (12). NACC was found to be the most

potent compound of this series against melanoma cells through inducing apoptosis rather than affecting the cell cycle (12). However, how apoptosis is triggered by NACC in melanoma cells remains unknown. The aims of the present study were to investigate the events involved in NACC-induced apoptosis and to elucidate the possible mechanism of action of NACC as an apoptosis inducer in melanoma cells. In addition, *in vitro* migration assays were performed to determine whether NACC is able to inhibit the migration of melanoma cells.

Materials and methods

Materials. NACC was synthesized in our laboratory according to a previously published method (12) and prepared as a 100 mM stock solution in dimethylsulphoxide (DMSO) for cell-based assays. Fetal bovine serum (FBS), RPMI-1640 growth medium, phosphate-buffered saline (PBS), penicillin/streptomycin solution and 0.25% trypsin-EDTA solution were purchased from Gibco Life Technologies (Grand Island, NY, USA). Fluo-3AM probe, mitochondria isolating kit, ROS kit, JC-1 kit and caspase-3, -8 and -9 kits were from Beyotime (Haimen, Jiangsu, China). EDTA disodium salt, sodium chloride, sodium dodecyl sulfate (SDS), glycine, 2-amino-2-(hydroxymethyl)propane-1,3-diol hydrochloride (Tris-HCl), Tween-20 and phenylmethanesulphonyl fluoride (PMSF) were purchased from Sigma-Aldrich Chemical Co. (Milwaukee, WI, USA). BD Pharmingen™ fluorescein isothiocyanate (FITC) Annexin V apoptosis detection kit I was from BD Biosciences (San Jose, CA, USA). Antibodies against Bcl-2, Bax, Bad, Mcl-1, Cyto *c*, p53, β-actin and horseradish peroxidase (HRP)-conjugated secondary antibodies were purchased from Cell Signaling Technology, Inc. (Beverly, MA, USA). Pierce® ECL Plus kit was purchased from Lumigen, Inc. (Southfield, MI, USA). Other reagents were obtained in their highest purity grade available commercially.

Cell line and culture conditions. Human melanoma cell line UACC-62 was a kind gift from Dr Xiangming Guan of South Dakota State University, USA. The melanoma cells were cultured at 37˚C in a humidified atmosphere of 5% CO_2 in RPMI-1640 medium supplemented with 10% FBS, 100 U/ml of penicillin and 100 μg/ml of streptomycin.

Apoptotic assay by flow cytometry. UACC-62 cells were seeded at densities of 10,000 or 30,000 cells/well in 6-well plates for the 3- and 5-day treatment, respectively. After a 24-h attachment at 37˚C, UACC-62 cells were treated with growth medium containing various concentrations of NACC. After the 3- or 5-day treatment, the treated and untreated cells were collected by trypsinization. Subsequently, Annexin V/propidium iodide (PI) staining was performed using the BD Pharmingen™ FITC Annexin V apoptosis detection kit I according to the manufacturer's instruction. The samples were analyzed with a Beckman Coulter flow cytometer.

Drug treatment for western blotting and caspase activity assays. UACC-62 cells were seeded into 100-mm culture dishes at densities of $1.5x10^5$/dish and $4.5x10^5$/dish for the 3- and 5-day treatment, respectively. The cells were allowed to attach for 24 h followed by treatment with either growth medium with 0.025% DMSO as control or NACC (1, 5 and 25 μM) for 3 or 5 days.

Determination of caspase activity. Activities of caspase-3, -8 and -9 were determined using caspase-3, -8 and -9 colorimetric assay kits from Beyotime as previously described by Cheng *et al* (13) with minor modifications. Briefly, UACC-62 cells were treated with NACC for 3 days as described above. The cells were collected and washed twice with PBS and then lysed for 15 min on ice in lysis buffer. The lysates were centrifuged at 16,000 x g for 15 min at 4˚C, and the supernatant was collected. Lysates were incubated with caspase-3, -8 and -9 substrates separately in reaction buffer at 37˚C for 1 h and their absorbance was recorded at 405 nm using a Multiskan Spectrum microplate reader (Thermo Scientific). The protein concentrations of the lysates were determined by the Bradford method.

Western blotting. The UACC-62 cells were treated with NACC as described above and then lysed in RIPA lysis buffer. The protein concentrations were determined by bicinchoninic acid (BCA) method. Aliquots of 25-80 μg protein were fractionated in 12.5 and 15% sodium dodecyl sulfate polyacrylamide gel (SDS-PAGE) under reducing conditions and then transferred to polyvinylidene fluoride (PVDF) membranes. After blocking with 5% non-fat milk, the membranes were probed with the appropriate dilution of primary antibodies followed by appropriate HRP conjugated secondary antibody. The resulting conjugates were visualized using Pierce® ECL Plus kit in a ChemiDoc XPS system (Bio-Rad Laboratories, Inc., Hercules, CA, USA).

Release of Cyto c. The cell homogenate containing cytosolic Cyto *c* released from mitochondria was generated by removing the intact mitochondria using a mitochondria isolating kit following the manufacturer's protocol. In brief, the UACC-62 cells were treated with or without NACC as described above for western blotting. The cells were harvested by trypsinization and rinsed once with cold PBS. The samples were centrifuged at 600 x g for 5 min at 4˚C and then the cell pellets were resuspended in mitochondria isolation buffer containing 1 mM PMSF. The cells were gently homogenized in a glass homogenizer avoiding breakage of the mitochondria. The homogenate was centrifuged at 600 x g for 10 min at 4˚C and the supernatants were centrifuged again at 11,000 x g for 10 min at 4˚C. The supernatants containing the cytosolic fraction were collected, and the protein concentration was determined by the BCA assay. The release of the cytosolic Cyto *c* was tested by western blotting using 25 μg protein as obtained above.

Flow cytometric analysis of mitochondrial membrane potential ($\Delta\psi_m$). JC-1 staining was performed to measure the changes in in $\Delta\psi_m$ in UACC-62 cells. The cells were seeded at densities of 16,000 or 48,000 cells/well in 6-well plates for the 3- and 5-day treatment, respectively. After a 24-h attachment, the cells were treated with NACC (0, 1, 5 and 25 μM) for various time periods. After the treatment, the cells were harvested by trypsinization and incubated with JC-1 (5 μg/ml) in JC-1 staining buffer for 20 min at 37˚C. $\Delta\psi_m$ was monitored by determining the relative amounts of

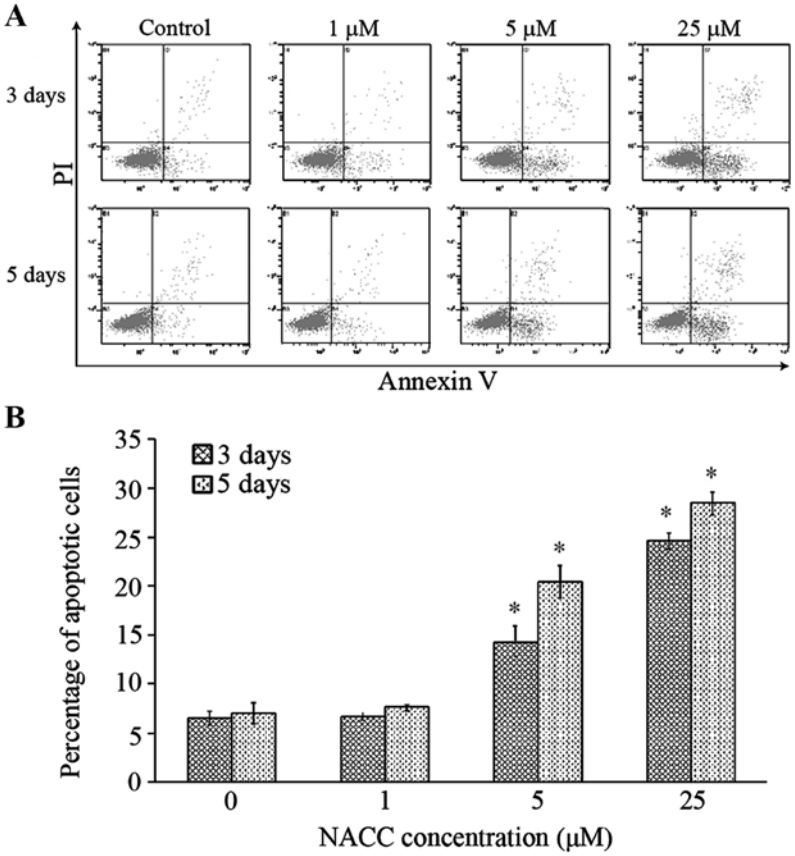

Figure 1. Effects of NACC on the induction of apoptosis in UACC-62 cells. UACC-62 cells were treated with various concentrations of NACC for 3 and 5 days. (A) The cells were stained with Annexin V and PI followed by flow cytometric analysis. (B) The percentages of apoptotic cells are presented following the 3-day and 5-day treatment. Results are presented as the mean ± SD of three independent experiments. *P<0.05 indicates statistical significance in the NACC-treated groups as compared to the controls.

dual emissions from mitochondrial JC-1 monomers (green) or aggregates (red) using a Beckman Coulter flow cytometer. At high $\Delta\psi_m$, JC-1 forms aggregates with intense red fluorescence, and JC-1 remains in the monomeric form at low $\Delta\psi_m$, which shows green fluorescence. For a positive control, the cells were incubated with 50 μM of the protonophore carbonyl cyanide *m*-chlorophenylhydrazone (CCCP), for 30 min at 37˚C followed by JC-1 staining as described above.

ROS production. ROS production induced by NACC was evaluated using the cell-permeative probe DCFH-DA. Upon entry into the cytoplasm, this probe is cleaved by cellular esterase and oxidized by ROS to yield green fluorescence. Briefly, UACC-62 cells were plated in 12-well plates at a density of 60,000 cells/well. After a 24-h attachment, the cells were treated with NACC at concentrations of 0, 1, 5 and 25 μM for 4 h followed by incubation with 10 μM DCFH-DA in FBS-free growth medium at 37˚C for 20 min. For a positive control, the cells were treated with 50 μM of Rosup at 37˚C for 20 min followed by DCFH-DA staining. The cells were washed with PBS three times and then the green fluorescence intensity was compared by the fluorescent images captured with a Nikon Ti-S fluorescent microscope.

Microscopy analysis of cytosolic calcium concentration in the UACC-62 cells. The cytosolic calcium concentrations were monitored using Fluo-3 acetoxymethyl (AM) probe as described by Gong *et al* (14). In brief, the cultured UACC-62 cells at a density of 80,000 cells/well in a 12-well plate were treated with various concentrations of NACC for 6 h. The cells were then incubated in full growth medium containing 5 μM Fluo-3 AM at 37˚C for 45 min. The probe-loaded cells were rinsed with PBS for 3 times and the green fluorescent images were captured using a Nikon Ti-S fluorescence microscope.

Mitochondrial PTP opening assay. PTP opening assay was performed using calcein-AM dye as described by Gautier *et al* (15). In brief, UACC-62 cells were seeded at densities of 8,000 or 24,000 cells/well in 12-well plates for the 3- and 5-day treatment, respectively. After a 24-h attachment at 37˚C, the cells were treated with growth medium containing various concentrations of NACC. After the 3- or 5-day treatment, the cells were washed with Hank's Balanced Salt Solution (HBSS) 1X and then loaded with calcein-AM (1 μM) with or without $CoCl_2$ (1 mM) both in HBSS 1X at 37˚C for 20 min. The cells were washed three times with HBSS 1X and the fluorescent images were captured with a Nikon Ti-S fluorescence microscope.

Real-time monitoring of cellular migration. The migration assays were performed on an xCELLigence system from ACEA Biosciences Inc. (San Diego, CA, USA) using CIM-16 plates. The experiments were conducted as described

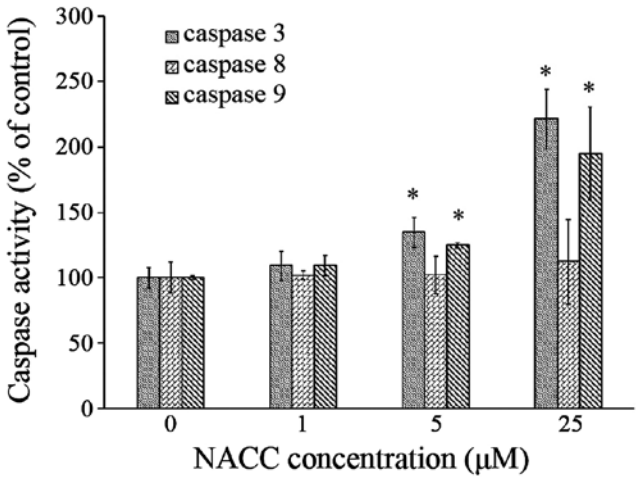

Figure 2. The effects of NACC on caspase activities in the UACC-62 cells. UACC-62 cells were treated with various concentrations of NACC for 3 days as described in Materials and methods. The cells were lysed and the caspase activities were determined by spectrophotometry. Results are presented as the mean ± SD of three independent experiments. *P<0.05 indicates statistical significance in the NACC-treated groups as compared to the controls.

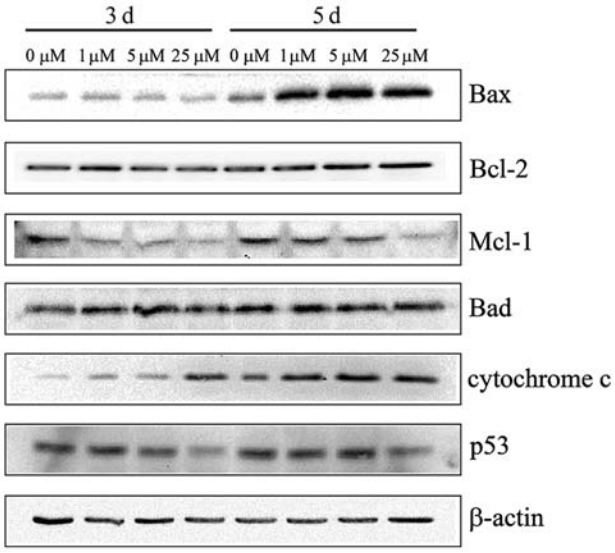

Figure 3. The effects of NACC on apoptosis-associated proteins in UACC-62 cells. The cells were treated with NACC (0, 1, 5 and 25 μM) for 3 or 5 days and then harvested. Western blotting was performed to examine the protein levels of Bax, Bcl-2, Mcl-1, Bad, Cyto *c* and p53 as described in Materials and methods. Images of the chemiluminescent detection of the blots, which are representative of three independent experiments, are shown. β-actin was used to verify equal loading of the samples.

by Eisenberg *et al* (16) with minor modifications. In brief, the wells of the bottom chamber were filled with 165 μl of medium containing 10% serum and then the top and bottom portions of the plates were assembled together. Serum-free media (30 μl) was added to the top chamber wells and the CIM-16 plates were allowed to equilibrate for 1 h at 37˚C in a 5% CO_2 incubator. The CIM-16 plates were then placed into the RTCA-DP instrument for baseline test. The UACC-62 cells were harvested by trypsinization and seeded to the top chamber wells at a density of 2,000 cells/well in 50 μl of serum-free medium. Another 50 μl of serum-free medium containing various concentrations of NACC was then added to the top chamber wells. The CIM-16 plates were allowed to incubate at room temperature for 30 min and placed into the RTCA-DP instrument for data collection. In addition, the cytotoxicity of NACC in UACC-62 cells was determined by the same xCELLigence system. In brief, the UACC-62 cells were seeded into E-plate 16 plates at a density of 2,000 cells/well followed by NACC treatment. The xCELLigence software was set to collect impedance data (cell index) every 15 min for 96 h.

Statistical analysis. Each experiment was performed in at least triplicate. Data were analyzed with INSTAT software (Graph Pad, San Diego, CA, USA). ANOVA followed by Tukey's post test was applied to compare the statistical difference between the NACC-treated groups and the untreated controls. P<0.05 was considered to indicate a statistically significant difference. Values are expressed as mean ± the standard deviation of the mean.

Results

NACC induces apoptosis in UACC-62 cells. NACC was previously found to be able to induce apoptosis in melanoma cells (12). In the present study, NACC-induced apoptosis was investigated at earlier treatment time points. FITC-conjugated Annexin V was utilized to detected the externalization of phosphatidylserine which is a marker of apoptosis. Combined with PI, an indicator of cell membrane destruction, the cell population undergoing apoptosis was quantified using flow cytometry. UACC-62 cells were treated with different concentrations of NACC for 3 or 5 days, and then the untreated and treated cells were collected followed by Annexin V/PI staining. Flow cytometric analysis was performed to detect the apoptosis in the UACC-62 cells induced by NACC. As shown in Fig. 1, NACC induced significant apoptosis in the UACC-62 cells following treatment with moderate (5 μM) and high (25 μM) concentrations of NACC in a dose- and time-dependent manner. NACC at 5 μM and 25 μM concentrations induced 14.2 and 24.6% and 20.4 and 28.5% apoptotic cells compared to that of 6.5 and 7.0% in the control samples following the 3- and 5-day treatment, respectively. The majority of the apoptotic cells were in the early stage of apoptosis.

Caspase activity is affected by NACC. To examine whether NACC plays a role in the activation of caspases and which apoptotic pathway is activated, we performed spectrophotometric analysis of the UACC-62 cell lysate to detect the activities of caspase-3, -8 and -9. The results showed that NACC significantly increased the activities of caspase-3 and caspase-9 in the melanoma cells in a dose-dependent manner but had no effect on the activity of caspase-8 (Fig. 2). These results demonstrated that the caspase cascade was activated during NACC-induced apoptosis and only the intrinsic pathway was involved in the NACC-induced apoptosis.

Western blotting. The apoptotic parameters, including protein levels of Bax, Bcl-2, Bad, Mcl-1 and Cyto *c* were investigated by western blotting to determine whether or not the intrinsic pathway is involved in the apoptosis induction in UACC-62 cells

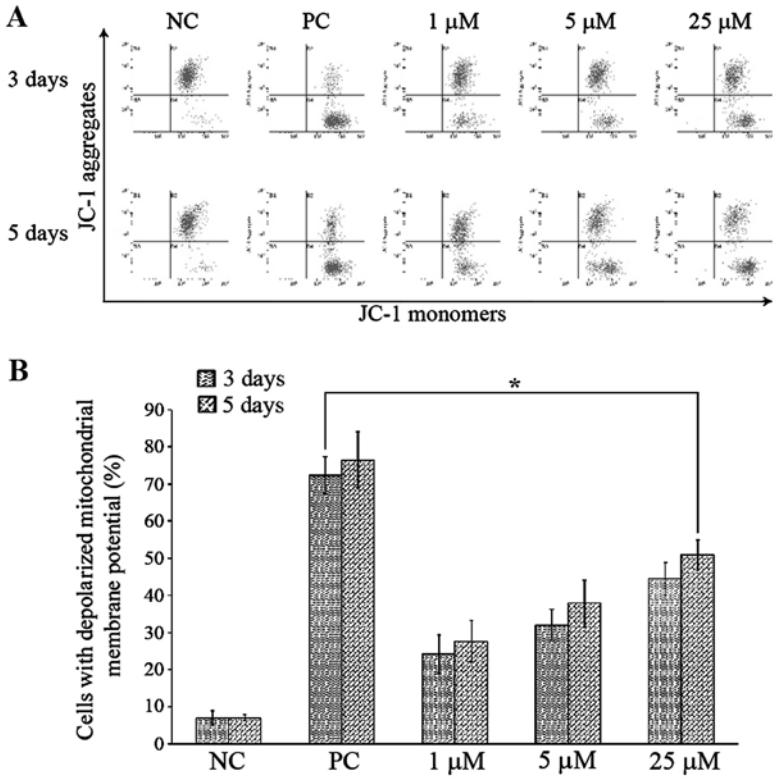

Figure 4. Effects of NACC on mitochondrial membrane potential in the UACC-62 cells as determined by flow cytometry. The cells were treated with NACC as indicated in 12-well plates for 3 or 5 days. After the treatment, the cells were harvested and stained with JC-1 (5 μg/ml) for 20 min at 37˚C. (A) Changes in mitochondrial membrane potential were monitored by determining the relative intensities of dual emissions from mitochondrial JC-1 monomers and aggregates by flow cytometry. (B) The percentages of the cells undergoing loss of mitochondrial membrane potential are presented. For a positive control, the cells were treated with 50 μM of the protonophore carbonyl cyanide *m*-chlorophenylhydrazone (CCCP) for 30 min at 37˚C followed by JC-1 staining. NC, negative control; PC, positive control. Results are presented as the mean ± SD of three independent experiments. *P<0.05 indicates statistical significance in the NACC-treated groups as compared to the controls.

by NACC (Fig. 3). Bax and Bad, the pro-apoptotic members of the Bcl-2 protein family, were investigated in this study. The results showed that Bax expression was upregulated following the 5-day treatment and that of Bad remained unchanged. NACC treatment showed downregulation of Mcl-1 expression and did not affect the Bcl-2 level. The results also showed that the level of cytosolic Cyto *c* increased in the NACC-treated melanoma cells (Fig. 3). In addition, the protein expression of p53 was investigated and the result showed that the p53 level remained unchanged following both 3- and 5-day treatment with low (1 μM) and medium (5 μM) concentrations of NACC. However, 25 μM of NACC slightly downregulated p53 in the UACC-62 cells. Thus, the increased Bax/Bcl-2 ratio and the downregulation of Mcl-1 were associated with the induction of apoptosis in the NACC-treated UACC-62 cells. As a result, Cyto *c* was released from the mitochondria to the cytosol.

NACC induces mitochondrial membrane potential ($\Delta\psi_m$) depletion. A decline in $\Delta\psi_m$ may be an early event in the process of cell death (6). JC-1 staining was performed to determine the changes in $\Delta\psi_m$ induced by NACC. JC-1 is a cationic dye that exhibits potential-dependent accumulation in mitochondria. During the loss of $\Delta\psi_m$, the fluorescence of the JC-1 dye shifts from red to green. The increase in green fluorescence indicates the loss of $\Delta\psi_m$ in the treated cells. Therefore, we studied the status of $\Delta\psi_m$ in the NACC-treated UACC-62 cells by JC-1 with flow cytometric analysis. As shown in Fig. 4, NACC treatment induced a dose- and time-dependent increase in the depletion of $\Delta\psi_m$. Concentrations of 1, 5 and 25 μM of NACC increased the percentage of cells undergoing $\Delta\psi_m$ depolarization from ~7.0% in the negative controls to 24.2, 32.0 and 44.4%, respectively following the 3-day treatment and 27.6, 38.8 and 50.9%, respectively, following the 5-day treatment. Positive controls treated with 50 μM of CCCP were conducted to ensure reliability of the analysis.

NACC increases ROS production in UACC-62 cells. To investigate whether ROS production is involved in NACC-induced apoptosis in UACC-62 cells, the generation of ROS in NACC-treated cells was probed by DCFH-DA fluorescent dye. The intensity of the green fluorescence which reflected the intracellular concentration of ROS was imaged by a fluorescence microscope. As shown in Fig. 5, NACC led to an increase in green fluorescence in NACC-treated UACC-62 cells indicating an increased ROS generation by NACC. Based on these observations, we concluded that NACC-induced apoptosis in part involved the production of ROS in UACC-62 cells.

Cytosolic calcium elevation in NACC-treated UACC-62 cells. To investigate whether NACC affects the cytosolic calcium concentration in UACC-62 cells, the intracellular calcium levels were probed by Fluo-3 AM. The cells were treated with NACC for 6 h and then stained with Fluo-3 AM fluorescent dye. The intensity of the green fluorescence which reflected

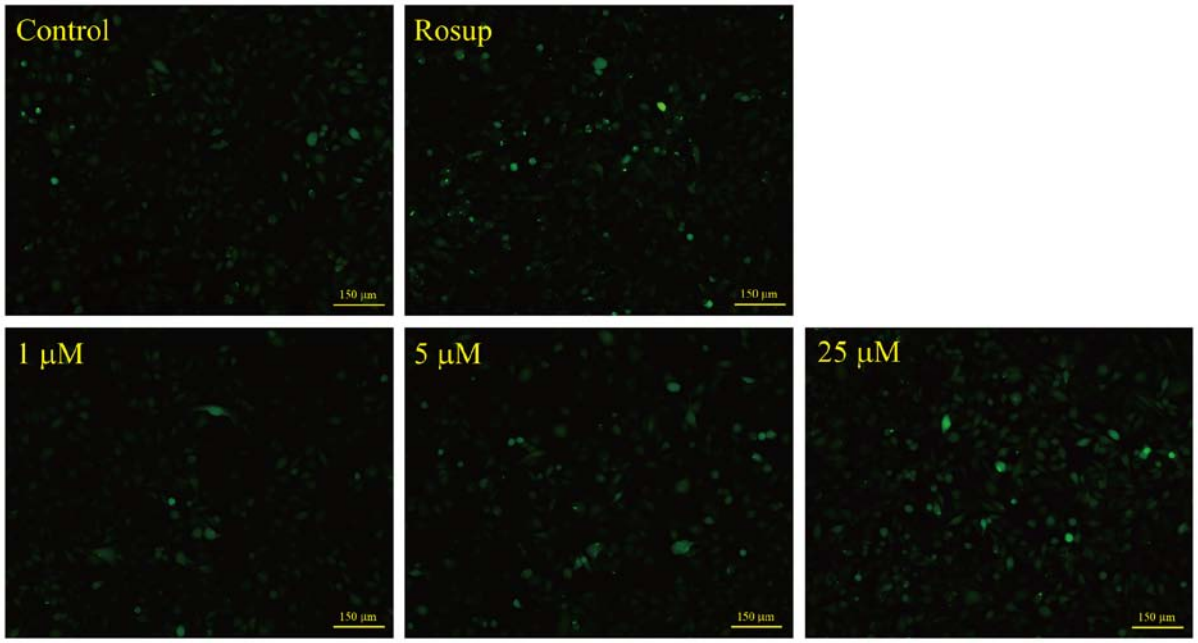

Figure 5. Effects of NACC on ROS production in the UACC-62 cells. ROS production induced by NACC was evaluated using the DCFH-DA probe which yields green fluorescence after it is cleaved by cellular esterase and oxidized by ROS. UACC-62 cells were treated with NACC in 12-well plates for 4 h followed by incubation with 10 μM DCFH-DA in FBS-free growth medium for 20 min at 37˚C. For a positive control, the cells were treated with 50 μM of Rosup for 20 min at 37˚C followed by DCFH-DA staining. The cells were washed with PBS, and the fluorescent images were captured with a fluorescence microscope. The data are derived from one of three independent experiments.

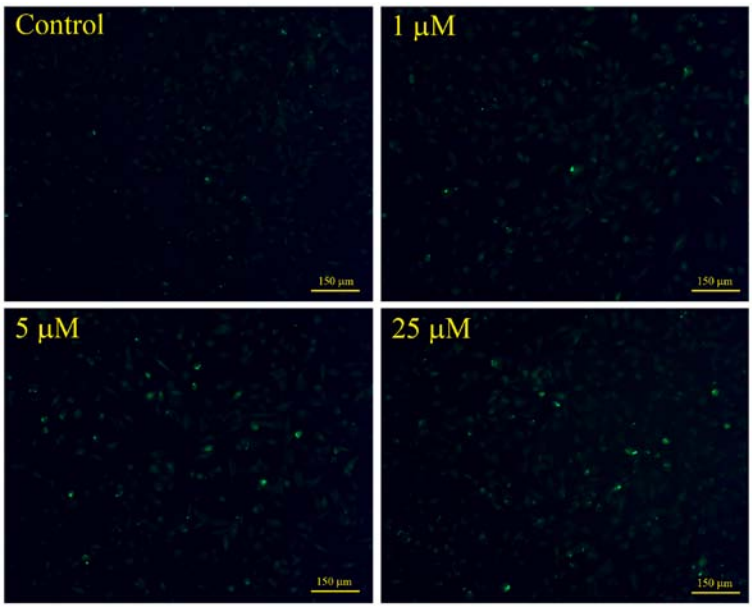

Figure 6. Effects of NACC on the cytosolic calcium concentration in the UACC-62 cells. The cytosolic calcium concentrations were monitored using Fluo-3 AM (cytoplasmic calcium indicator). UACC-62 cells were treated with 0, 1, 5 and 25 μM concentrations of NACC for 6 h. The cells were then loaded with Fluo-3 AM. The cells were rinsed with PBS, and fluorescent images were captured using a fluorescence microscope. The intensity of the green fluorescence reflects the cytosolic calcium concentrations. The data are derived from one of three independent experiments.

the intracellular free calcium concentrations was compared by the images captured by a fluorescence microscope. As shown in Fig. 6 NACC led to an increase in the green fluorescence in the NACC-treated UACC-62 cells indicating marked elevation of cytosolic calcium concentration induced by NACC.

Mitochondrial PTP opening. Since Cyto *c* release and a loss of mitochondrial membrane potential were observed in the NACC-treated melanoma cells, we evaluated opening of the mitochondrial PTP, which may regulate the Cyto *c* release across the mitochondrial inner membrane (17,18). We compared the opening of PTP in NACC-treated and untreated melanoma cells using the calcein AM fluorescence assay. Calcein-AM is a membrane permeable fluorophore that diffuses freely into all subcellular compartments including mitochondria. The AM group of the fluorophore is cleaved by ubiquitous intracellular

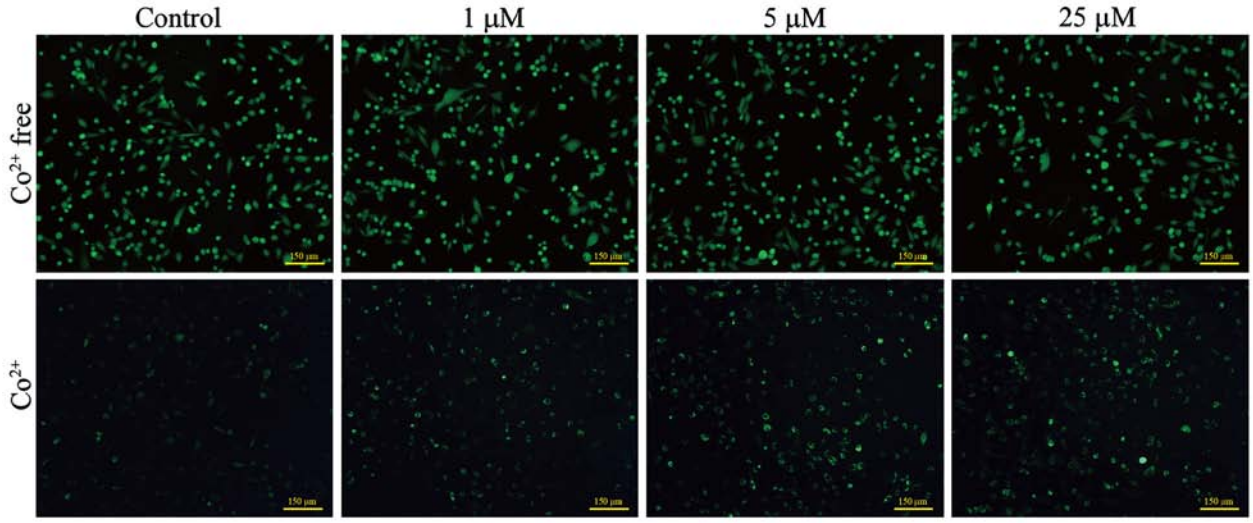

Figure 7. Effects of NACC on PTP opening. PTP opening assay was performed using calcein-AM dye as described by Gautier *et al* (15). In brief, UACC-62 cells were seeded at densities of 8,000 or 24,000 cells/well in 12-well plates for the 3- and 5-day treatment, respectively. After a 24-h attachment at 37˚C, the cells were treated with growth medium containing various concentrations of NACC. After the 3- or 5-day treatment, the cells were washed with HBSS 1X and then loaded with calcein-AM (1 μM) with or without $CoCl_2$ (1 mM) both in HBSS 1X for 20 min at 37˚C. The cells were washed three times with HBSS 1X and fluorescent images were captured with a Nikon Ti-S fluorescence microscope.

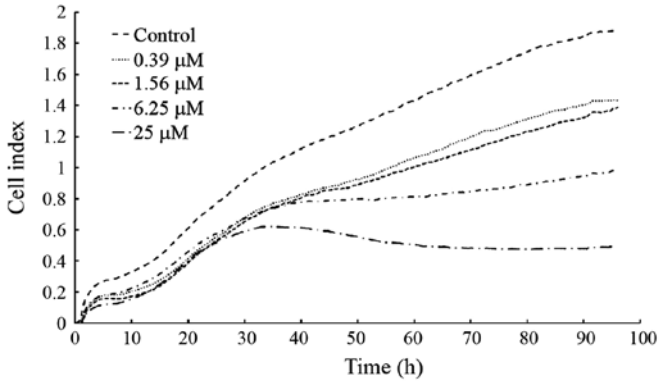

Figure 8. The effects of NACC on UACC-62 cell migration. UACC-62 cell migration was assessed using a CIM-16 plate with 8-μm pores. Medium containing 10% FBS was added to the lower chambers, and cells were seeded into the upper chamber at 2,000 cells/well in FBS-free medium. The CIM-16 plate was monitored every 15 min for 96 h. Data analysis was carried out using RTCA software 2.0. The experiments were repeated in replicates and three times independently. Each plot shows one of the triplicate experiments.

esterase. The hydrophilic calcein is then trapped within all subcellular compartments. The cells were then loaded with Co^{2+}, which quenches calcein fluorescence in all subcellular compartments except the mitochondrial matrix, since the inner mitochondrial membrane is the only Co^{2+}-impermeable intracellular membrane (15,19). During the opening of the PTP, Co^{2+} enters into mitochondria and quenches mitochondrial calcein fluorescence (20). Fig. 7 shows that the NACC treatment did not induce a decrease in green fluorescence which indicated that NACC did not trigger PTP opening in the UACC-62 cells.

NACC suppresses the migration of UACC-62 cells in vitro. The migration assay in UACC-62 cells was performed using an xCELLigence system. Cells seeded in the top chamber move through the microporous membrane into the bottom chamber containing FBS. Then the cells are able to adhere to the microelectrode sensors leading to an increase in cell index. The instrument provides real-time and successive detection of the total migrated cells. To ensure that the NACC-induced migration suppression was not caused by the cytotoxicity of NACC, parallel experiments were conducted in E-plate 16 plates instead of CIM-16 plates to determine the cytotoxicity in the UACC-62 cells. The results showed that the migratory ability of UACC-62 cells was significantly suppressed in a dose- and time-dependent manner (Fig. 8). The cell index curves of the control and NACC-treated cells separated at the very beginning of the experiments. Among the curves of migration, 25 μM NACC started to show inhibitory effects on migration at 25 h, and 6.25 μM NACC started to flatten the curve from ~40 h. The curves for low concentrations (1.56 and 0.39 μM) started to separate at ~50 h. The IC_{50} value of NACC on UACC-62 cell migration following the 96-h treatment was determined to be 4.93±2.64 μM based on three independent experiments. The cytotoxicity experiments showed that NACC at 0.39, 1.56, 6.25 and 25 μM inhibited 2.89±3.9, 7.35±1.75, 13.38±0.58 and 19.94±0.8% cell growth compared to the control following the 96-h treatment, respectively. Obviously, the cell growth inhibition rates were much lower than that of the migration inhibition rates induced by the same concentration of NACC, indicating that the suppression of NACC-induced migration was not caused by NACC-induced cytotoxicity.

Discussion

Malignant melanoma is well-known for its high therapeutic resistance resulting in failed clinical trials. At present, to the best of our knowledge, there are no efficacious therapies for malignant melanoma, and defective apoptotic pathways are thought to be one of the most important barriers in the treat-

ment of malignant melanoma (21,22). NACC was found to be an apoptosis-inducer in melanoma cells. Flow cytometric analysis revealed that NACC induced UACC-62 cell apoptosis in a dose- and time-dependent manner (Fig. 1). To shed more light on the apoptotic mechanism triggered by NACC, we investigated the underlying molecular mechanisms of NACC-induced apoptosis in melanoma cells.

It is well-known that the complex cascade of caspases is involved in the process of apoptotic cell death (23). Since caspases play important roles in the apoptotic process, involvement of the caspase cascade in NACC-induced UACC-62 cell apoptosis was investigated. There are at least two major pathways, intrinsic and extrinsic, initiated by caspase-8 and caspase-9, respectively. They in turn activate the caspase cascade in cells (23). The activities of caspase-3, an important effector caspase, and two initiator caspases, caspase-8 and caspase-9, were determined by photometric assays. The results showed that caspase-3 and -9 were significantly activated in the NACC-treated UACC-62 cells, however, the activity of caspase-8 remained unchanged. This indicated that only the intrinsic pathway of apoptosis was activated by NACC.

The intrinsic apoptotic pathway also called the mitochondrial apoptotic pathway is mediated by the interplay between anti-apoptotic and pro-apoptotic members of the Bcl-2 family (24,25). Bcl-2 family proteins are thought to play essential roles in the regulation of apoptotic execution of cells (26). In this study, we investigated the expression of Bcl-2 family proteins in UACC-62 cells treated with NACC. First of all, the expression levels of Bcl-2 and Bax, the most important members of the Bcl-2 family, were determined by western blotting in UACC-62 cells. The results showed that NACC upregulated Bax, a representative of the pro-apoptotic members (27), but did not affect the expression of Bcl-2. Mcl-1, an anti-apoptotic member of the Bcl-2 family which is extensively expressed in melanoma and contributes to melanoma's well-documented drug resistance and poor prognosis (28), was found to be downregulated in the NACC-treated melanoma cells. p53, a tumor suppressor, is at the center of an intricate protein network determining important cellular responses including apoptosis (29). The western blotting results showed that the wild-type p53 carried in the UACC-62 cells (30) was not found to be upregulated by NACC treatment indicating that NACC-induced apoptosis was p53-independent. All of these results suggest that NACC-induced apoptosis was initiated by an increased ratio of Bax/Bcl-2 and downregulation of Mcl-1. Moreover, another pro-apoptotic member Bad was found unaltered in the NACC-induced apoptosis. Accumulation of pro-apoptotic proteins on the mitochondrial outer membrane changes the mitochondrial membrane permeability and release of Cyto *c* from the mitochondria to the cytoplasm. Cyto *c* is a small hemeprotein normally absorbed at the outer aspect of the inner membrane of mitochondria and is an essential component of the electron transport chain. Cyto *c* activates the caspase-dependent or -independent apoptotic pathways and plays a central role in the caspase-dependent mitochondrial-mediated apoptotic pathway (17,31,32). The results of western blotting (Fig. 3) showed that Cyto *c* was released to the cytosol in the UACC-62 cells treated with NACC as a consequence of the regulation of Bax and Mcl-1 expression by NACC.

Mitochondria play a critical role in the regulation of apoptosis. The disruption of $\Delta\psi_m$ can mediate liberation of Cyto *c* into the cytosol (33). As shown in Fig. 4, NACC treatment caused depletion of $\Delta\psi_m$, and the percentage of the cells with depolarized mitochondria exposed to 1, 5 and 25 μM of NACC increased from 7.0 to 24.2%, 32.0 and 44.4% following a 3-day treatment and from 6.9 to 27.6%, 37.8 and 50.9% following a 5-day treatment, respectively. Mitochondria are also known as the major intracellular source of ROS. ROS participate as effective factors in apoptosis by disruption of mitochondrial membrane potential (34). When the generation of ROS is out of control, ROS are capable of inducing apoptosis (35). Increased ROS have been found to be implicated in the induction of apoptosis by promoting the release of Cyto *c* to facilitate caspase cascade activation (36). Changes in the level of ROS in UACC-62 cells were further assessed. The results showed that NACC generated ROS in UACC-62 cells. ROS generation could precede the depolarization of the mitochondrial membrane (37), which is one of the earliest events of apoptosis. We observed an increase in ROS production after a 4-h exposure of melanoma cells to NACC suggesting that the generation of ROS is an early event in NACC activity in treated melanoma cells. ROS generation by NACC could be one of the factors responsible for the disruption of mitochondrial membrane potential in the melanoma cells. Recently, we found that NACC is an irreversible inhibitor which is capable of inhibiting intracellular thioredoxin reductase (TrxR) in UACC-62 cells (38). It was reported by Fang *et al* (39) that TrxR inhibitor is able to induce ROS production in the presence of oxygen. Therefore, the observed ROS generation by NACC might be a consequence of the inhibition of intracellular TrxR in UACC-62 cells.

Sulofenur, the parent compound of NACC (40), was reported to be able to alter the mitochondrial membrane potential by elevation of cytosolic calcium concentration in human colon cancer cells (41). The cytosolic calcium level was assessed in the melanoma cells exposed to NACC for 6 h. A dramatic increase in cytosolic calcium was observed in the UACC-62 cells indicating that NACC had the same ability as sulofenur in the elevation of cytosolic calcium (Fig. 6). Mitochondrial membrane permeabilization is considerate as an important hallmark of early apoptosis. Elevation of the cytosolic calcium concentration may play a role in induction of PTP (42). Mitochondrial permeability transition is thought to be regulated by the opening of the PTP (43). However, the role of PTP in the mitochondrial pathway of apoptosis is still controversial (42,44). In the present study, opening of the PTP was assessed in the UACC-62 cells treated with NACC. Notably, the results showed that NACC did not induce the opening of the PTP (Fig. 7). PTP putatively consists of the voltage dependent anion channel (VDAC) in the outer mitochondrial membrane (OMM), the adenine nucleotide translocase (ANT) in the inner mitochondrial membrane (IMM) and a mitochondrial matrix protein cyclophilin D (CyP-D) (44). It has been reported that the pro-apoptotic protein Bax is able to interact with VDAC and ANT to accelerate the opening of PTP (42,44,45). Yet, the PTP opening was not triggered by Bax upregulation in the UACC-62 cells. It is known that Bax can be activated to form pores in the OMM and dictate mitochondrial outer membrane permeabilization (MOMP) which triggers Cyto *c* release from

the intramembrane space and subsequent apoptosis (46). Our results showed that in the UACC-62 cells, NACC induced Cyto *c* release via MOMP by upregulated Bax and was not PTP-dependent. The results were consistent with a previous report which found that the regulatory release of Cyto *c* from mitochondria could occur independently through regulation of PTP opening (47).

Melanomas are highly metastatic resulting in poor therapeutic outcomes and a low survival rate (48). Thus, suppression of cancer cell metastasis is one of the key factors in cancer therapy. Migration is one of the key steps of metastasis. In the present study, we investigated the suppressive ability of NACC against the migration of the UACC-62 cell line. The IC_{50} value of NACC on the migration in UACC-62 cells following a 96-h treatment was determined to be 4.93±2.64 μM implying that NACC has promising anti-metastatic activity against melanoma cells. The thioredoxin system has been shown to mediate the ability of cell migration and tissue invasion of melanoma (49,50). As previously mentioned, NACC is an irreversible inhibitor of TrxR and is capable of inhibiting intracellular TrxR. Therefore, inhibition of the activity of TrxR which is the major component of the thioredoxin system, may contribute to the suppressive effect of NACC on the migration in UACC-62 cells. How the thioredoxin system is involved in tumor cell migration and invasion is not yet clear. The impacts of NACC on other steps of metastasis and its mechanism of action will be further investigated in future studies.

In conclusion, NACC has the capability of inducing mitochondrial-mediated apoptosis, which is well regulated by the caspase enzymes. Moreover, the active role of mitochondria in NACC-induced programmed cell death was confirmed by depletion of the mitochondrial membrane potential, release of Cyto *c*, generation of ROS, cytosolic calcium elevation and regulation of pro-apoptotic and anti-apoptotic proteins (Bax/Bcl-2 and Mcl-1). The results suggest that NACC is a promising anti-melanoma agent that is not only capable of triggering apoptosis via the mitochondrial-dependent pathway, but is also able to suppress the migration of melanoma cells.

Acknowledgements

The present study was supported by the National Natural Science Foundation of China (81202553), Medical and Health Science Foundation of Zhejiang Province (2012KYA034) and Zhejiang Key Laboratory of Diagnosis and Treatment Technology on Thoracic Oncology (Lung and Esophagus).

References

1. Markovic SN, Erickson LA, Rao RD, Weenig RH, Pockaj BA, Bardia A, Vachon CM, Schild SE, McWilliams RR, Hand JL, *et al*; Melanoma Study Group of the Mayo Clinic Cancer Center: Malignant melanoma in the 21st century, part 1: Epidemiology, risk factors, screening, prevention, and diagnosis. Mayo Clin Proc 82: 364-380, 2007.
2. Gogas HJ, Kirkwood JM and Sondak VK: Chemotherapy for metastatic melanoma: Time for a change? Cancer 109: 455-464, 2007.
3. Bergomi M, Pellacani G, Vinceti M, Bassissi S, Malagoli C, Alber D, Sieri S, Vescovi L, Seidenari S and Vivoli R: Trace elements and melanoma. J Trace Elem Med Biol 19: 69-73, 2005.
4. de Vries E, Houterman S, Janssen-Heijnen ML, Nijsten T, van de Schans SA, Eggermont AM and Coebergh JW: Up-to-date survival estimates and historical trends of cutaneous malignant melanoma in the south-east of The Netherlands. Ann Oncol 18: 1110-1116, 2007.
5. Yang J, Amiri KI, Burke JR, Schmid JA and Richmond A: BMS-345541 targets inhibitor of kappaB kinase and induces apoptosis in melanoma: Involvement of nuclear factor kappaB and mitochondria pathways. Clin Cancer Res 12: 950-960, 2006.
6. Hu WP, Yu HS, Sung PJ, Tsai FY, Shen YK, Chang LS and Wang JJ: DC-81-Indole conjugate agent induces mitochondria mediated apoptosis in human melanoma A375 cells. Chem Res Toxicol 20: 905-912, 2007.
7. Kim R: Recent advances in understanding the cell death pathways activated by anticancer therapy. Cancer 103: 1551-1560, 2005.
8. Jana S, Paul S and Swarnakar S: Curcumin as anti-endometriotic agent: Implication of MMP-3 and intrinsic apoptotic pathway. Biochem Pharmacol 83: 797-804, 2012.
9. Jiang X and Wang X: Cytochrome *c*-mediated apoptosis. Annu Rev Biochem 73: 87-106, 2004.
10. Estaquier J, Vallette F, Vayssiere JL and Mignotte B: The mitochondrial pathways of apoptosis. Adv Exp Med Biol 942: 157-183, 2012.
11. Rizzuto R, Pinton P, Ferrari D, Chami M, Szabadkai G, Magalhães PJ, Di Virgilio F and Pozzan T: Calcium and apoptosis: Facts and hypotheses. Oncogene 22: 8619-8627, 2003.
12. Chen W, Seefeldt T, Young A, Zhang X and Guan X: Design, synthesis and biological evaluation of *N*-acetyl-*S*-(*p*-chloro phenylcarbamoyl)cysteine and its analogs as a novel class of anticancer agents. Bioorg Med Chem 19: 287-294, 2011.
13. Cheng J, Tang W, Su Z, Guo J, Tong L and Wei Q: Calcineurin subunit B promotes TNF-alpha-induced apoptosis by binding to mitochondria and causing mitochondrial Ca^{2+} overload. Cancer Lett 321: 169-178, 2012.
14. Gong YY, Si XM, Lin L and Lu J: Mechanisms of cholecystokinin-induced calcium mobilization in gastric antral interstitial cells of Cajal. World J Gastroenterol 18: 7184-7193, 2012.
15. Gautier CA, Giaime E, Caballero E, Núñez L, Song Z, Chan D, Villalobos C and Shen J: Regulation of mitochondrial permeability transition pore by PINK1. Mol Neurodegener 7: 22, 2012.
16. Eisenberg MC, Kim Y, Li R, Ackerman WE, Kniss DA and Friedman A: Mechanistic modeling of the effects of myoferlin on tumor cell invasion. Proc Natl Acad Sci USA 108: 20078-20083, 2011.
17. Ichas F and Mazat JP: From calcium signaling to cell death: Two conformations for the mitochondrial permeability transition pore. Switching from low- to high-conductance state. Biochim Biophys Acta 1366: 33-50, 1998.
18. Garrido C, Galluzzi L, Brunet M, Puig PE, Didelot C and Kroemer G: Mechanisms of cytochrome c release from mitochondria. Cell Death Differ 13: 1423-1433, 2006.
19. Petronilli V, Miotto G, Canton M, Colonna R, Bernardi P and Di Lisa F: Imaging the mitochondrial permeability transition pore in intact cells. Biofactors 8: 263-272, 1998.
20. Hüser J, Rechenmacher CE and Blatter LA: Imaging the permeability pore transition in single mitochondria. Biophys J 74: 2129-2137, 1998.
21. Tsao H, Chin L, Garraway LA and Fisher DE: Melanoma: From mutations to medicine. Genes Dev 26: 1131-1155, 2012.
22. Li X, Wu D, Shen J, Zhou M and Lu Y: Rapamycin induces autophagy in the melanoma cell line M14 via regulation of the expression levels of Bcl-2 and Bax. Oncol Lett 5: 167-172, 2013.
23. Sun J, Yu CH, Zhao XL, Wang Y, Jiang SG and Gong XF: Econazole nitrate induces apoptosis in MCF-7 cells via mitochondrial and caspase pathways. Iran J Pharm Res 13: 1327-1334, 2014.
24. Czabotar PE, Lessene G, Strasser A and Adams JM: Control of apoptosis by the BCL-2 protein family: Implications for physiology and therapy. Nat Rev Mol Cell Biol 15: 49-63, 2014.
25. Bi MC, Rosen R, Zha RY, McCormick SA, Song E and Hu DN: Zeaxanthin induces apoptosis in human uveal melanoma cells through Bcl-2 family proteins and intrinsic apoptosis pathway. Evid Based Complement Alternat Med 2013: 205082, 2013.
26. Matsumoto A, Isomoto H, Nakayama M, Hisatsune J, Nishi Y, Nakashima Y, Matsushima K, Kurazono H, Nakao K, Hirayama T, *et al*: *Helicobacter pylori* VacA reduces the cellular expression of STAT3 and pro-survival Bcl-2 family proteins, Bcl-2 and Bcl-XL, leading to apoptosis in gastric epithelial cells. Dig Dis Sci 56: 999-1006, 2011.

27. Robertson JD and Orrenius S: Molecular mechanisms of apoptosis induced by cytotoxic chemicals. Crit Rev Toxicol 30: 609-627, 2000.
28. Liu Y, Xie M, Song T, Sheng H, Yu X and Zhang Z: A novel BH3 mimetic efficiently induces apoptosis in melanoma cells through direct binding to anti-apoptotic Bcl-2 family proteins, including phosphorylated Mcl-1. Pigment Cell Melanoma Res 28: 161-170, 2015.
29. Amaral JD, Xavier JM, Steer CJ and Rodrigues CM: The role of p53 in apoptosis. Discov Med 9: 145-152, 2010.
30. Bykov VJ, Issaeva N, Selivanova G and Wiman KG: Mutant p53-dependent growth suppression distinguishes PRIMA-1 from known anticancer drugs: A statistical analysis of information in the National Cancer Institute database. Carcinogenesis 23: 2011-2018, 2002.
31. Pradelli LA, Bénéteau M and Ricci JE: Mitochondrial control of caspase-dependent and -independent cell death. Cell Mol Life Sci 67: 1589-1597, 2010.
32. Li P, Nijhawan D, Budihardjo I, Srinivasula SM, Ahmad M, Alnemri ES and Wang X: Cytochrome c and dATP-dependent formation of Apaf-1/caspase-9 complex initiates an apoptotic protease cascade. Cell 91: 479-489, 1997.
33. Luo Y, Li X, Huang X, Wong YS, Chen T, Zhang Y and Zheng W: 1,4-Diselenophene-1,4-diketone triggers caspase-dependent apoptosis in human melanoma A375 cells through induction of mitochondrial dysfunction. Chem Pharm Bull (Tokyo) 59: 1227-1232, 2011.
34. Zamzami N, Marchetti P, Castedo M, Decaudin D, Macho A, Hirsch T, Susin SA, Petit PX, Mignotte B and Kroemer G: Sequential reduction of mitochondrial transmembrane potential and generation of reactive oxygen species in early programmed cell death. J Exp Med 182: 367-377, 1995.
35. Su YT, Chang HL, Shyue SK and Hsu SL: Emodin induces apoptosis in human lung adenocarcinoma cells through a reactive oxygen species-dependent mitochondrial signaling pathway. Biochem Pharmacol 70: 229-241, 2005.
36. Kagan VE, Tyurin VA, Jiang J, Tyurina YY, Ritov VB, Amoscato AA, Osipov AN, Belikova NA, Kapralov AA, Kini V, *et al*: Cytochrome c acts as a cardiolipin oxygenase required for release of proapoptotic factors. Nat Chem Biol 1: 223-232, 2005.
37. Rogalska A, Koceva-Chyła A and Jóźwiak Z: Aclarubicin-induced ROS generation and collapse of mitochondrial membrane potential in human cancer cell lines. Chem Biol Interact 176: 58-70, 2008.
38. Chen W, Jiang Z, Lin N, Zheng Z, Chen Z, Zhang X and Guan X: Evaluation of N-acetyl-S-(p-chlorophenylcarbamoyl)cysteine as an irreversible inhibitor of mammalian thioredoxin reductase1. J Enzyme Inhib Med Chem 17: 1-7, 2015.
39. Fang J, Lu J and Holmgren A: Thioredoxin reductase is irreversibly modified by curcumin: A novel molecular mechanism for its anticancer activity. J Biol Chem 280: 25284-25290, 2005.
40. Guan X, Hoffman BN, McFarland DC, Gilkerson KK, Dwivedi C, Erickson AK, Bebensee S and Pellegrini J: Glutathione and mercapturic acid conjugates of sulofenur and their activity against a human colon cancer cell line. Drug Metab Dispos 30: 331-335, 2002.
41. Phelps PC, Jain PT, Berezesky IK, Boder GB and Trump BF: Sulofenur cytotoxicity and changes in cytosolic calcium and mitochondrial membrane potential in human colon adenocarcinoma cell lines. Cancer Lett 88: 27-35, 1995.
42. Gerasimenko JV, Gerasimenko OV, Palejwala A, Tepikin AV, Petersen OH and Watson AJ: Menadione-induced apoptosis: Roles of cytosolic Ca(2+) elevations and the mitochondrial permeability transition pore. J Cell Sci 115: 485-497, 2002.
43. Nakagawa T, Shimizu S, Watanabe T, Yamaguchi O, Otsu K, Yamagata H, Inohara H, Kubo T and Tsujimoto Y: Cyclophilin D-dependent mitochondrial permeability transition regulates some necrotic but not apoptotic cell death. Nature 434: 652-658, 2005.
44. Suh DH, Kim MK, Kim HS, Chung HH and Song YS: Mitochondrial permeability transition pore as a selective target for anti-cancer therapy. Front Oncol 3: 41, 2013.
45. Marzo I, Brenner C, Zamzami N, Jürgensmeier JM, Susin SA, Vieira HL, Prévost MC, Xie Z, Matsuyama S, Reed JC, *et al*: Bax and adenine nucleotide translocator cooperate in the mitochondrial control of apoptosis. Science 281: 2027-2031, 1998.
46. Chipuk JE, Bouchier-Hayes L and Green DR: Mitochondrial outer membrane permeabilization during apoptosis: The innocent bystander scenario. Cell Death Differ 13: 1396-1402, 2006.
47. Toriumi K, Oma Y, Mimoto A, Futai E, Sasagawa N, Turk B and Ishiura S: Polyalanine tracts directly induce the release of cytochrome c, independently of the mitochondrial permeability transition pore, leading to apoptosis. Genes Cells 14: 751-757, 2009.
48. Bonaventure J, Domingues MJ and Larue L: Cellular and molecular mechanisms controlling the migration of melanocytes and melanoma cells. Pigment Cell Melanoma Res 26: 316-325, 2013.
49. Mahmood DF, Abderrazak A, El Hadri K, Simmet T and Rouis M: The thioredoxin system as a therapeutic target in human health and disease. Antioxid Redox Signal 19: 1266-1303, 2013.
50. Arnér ES and Holmgren A: The thioredoxin system in cancer. Semin Cancer Biol 16: 420-426, 2006.